Journal of Computational Applied Mechanics 2024, 55(2): 275-288

DOI: 10.22059/JCAMECH.2024.374576.1024

RESEARCH PAPER

Vibration analysis of the Gamma-Ray element in the ELI-NP interaction chamber (IC)

Sorin Vlase[a,b], Calin Itu[a], Marin Marin[c,d,*], Maria Luminta Scutaru[a], Florin Sabou[e], Radu Necula[e]

[a] *Department of Mechanical Engineering, Transilvania University of Brasov, Romania*
[b] *Technical Sciences Academy of Romania, Calea Victoriei, Bucharest, Romania*
[c] *Department of Mathematics and Computer Science, Transilvania University of Brasov, Romania*
[d] *Academy of Romanian Scientists, Ilfov Street 3, 050045 Bucharest, Romania*
[e] *Department of Medical and Surgical Specialties, Transilvania University of Brasov, Romania*

Abstract

The influence of vibrations on the position of the target in the interaction chamber of the ELI-NP facility represents an important element in any experiment with gamma beam rays. Also, several detection systems are provided around the interaction chamber for tracking the nuclear reactions that occur inside the interaction chamber. They are fixed with very high precision in relation to the interaction chamber. In addition to tracking the gamma ray beam, it must to know with great precision the position of the sample holder and of these detectors placed in laboratory. The precision required for a gamma-ray experiment is determined by the size of the studied material. If there is enough target material, then the precision is not important, but if we have a very small amount of material, then precision becomes significant. For a common experiment, accuracy is considered satisfactory for a value of 2μm. The paper analyzes the influence of anthropogenic and natural vibrations on the position of the target, located at the end of a guide beam.

Keywords: Vibration analysis; ELI-NP; gamma-ray; Interaction Chamber; guide element

1. Introduction

In the work, the beam that serves to guide the gamma beam used inside the Interaction Chamber (IC) at ELI-NP (Extreme Light Infrastructure–Nuclear Physics) project is analyzed. All the equipment, including the interaction room in which this element studied in the paper is located, are placed on the inertial platform. All equipment, including this beam, are extremely sensitive and precise and an efficient anti-vibration system must be ensured, against the human (anthropic) and natural (earthquakes) factors. The ELI-NP project consists in the realization of an advanced source of 10 MeV Gamma rays. A high-intensity laser (up to 1024 W/cm^2) will also be created. Details of this project can be found in [1, 2].

* Corresponding author. Tel.: +0-000-000-0000 ; fax: +0-000-000-0000 .
E-mail address: m.marin@unitbv.ro

The expected gamma source that was realized in this project offers the support of some important experiments in nuclear resonance fluorescence (NRF), see [3, 4]. The precision and small size of the produced beam as well as the possibility to position it extremely precisely creates the prerequisites for obtaining spectacular results in the field. In this sense, the positioning system, which is part of and analyzed in this work, must be designed and made very precisely, which is why they are studied in this work. Obviously, in order to achieve extremely precise positioning, a special isolation is necessary against vibrations and which are produced by some anthropic activities or some natural phenomena (earthquakes). This can be achieved through a judicious design and realization of the platform on which the equipment stands, which is unique engineering achievement in the field.

If are considered the high costs involved in the realization of this project and the high performance that it has to fulfill, in the design stage the best possible modeling is done to choose a solution that satisfies the purpose with the lowest costs. Common sources of vibration that occur are due to usual activities. They are varied and due to the daily activities, that take place (public or industrial transport around the building or other activities that are carried out continuously on a current basis). The main and most dangerous source of natural vibrations is earthquake. For the area where the institute is located, represents a rare phenomenon over a period of approximately 40-50 years when it manifests dramatically. That is why a calculation to vibrations of this sensitive beam is absolutely necessary.

In the paper we will present a study on the dynamic response of the IC for the ELI-NP particle detector based on an excitation from the base. Taking into account the fact that the vibration of the system can significantly influence the direction of the very narrow gamma-ray beam that must reach a target subjected to analysis, a very good knowledge of the dynamic response of the element that directs the light beam of rays is necessary [5-7].

The interaction chamber (CI) of the ELIADE particle detector and the CCD (Charged *Coupled Device)* camera forms the so-called IC-NRF system in Figure 1(Internal Chamber – Nuclear Resonance Fluorescence) with the role of identifying the gamma beam, and the element that directs this beam must comply with the structural and functional requirements imposed by the specifications.

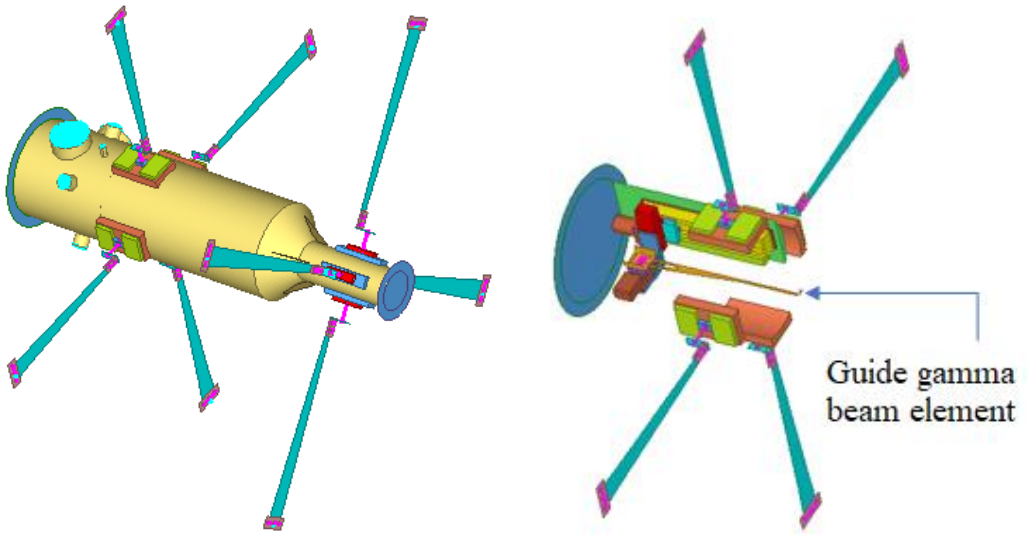

a) b)

Fig.1: IC-NRF system

As functional requirements, the IC-NRF system must:

- ✓ to hold a target of a solid, liquid or gaseous material. This target will be hit by gamma beams,
- ✓ to be able to maintain vacuum conditions at a pressure of 10^{-3} mbar,
- ✓ can be integrated into the global ELIADE structure that holds a set of Ge detectors used in the NRF (Nuclear *Resonance Fluorescence*) experiments,
- ✓ to be able to ensure the mechanical alignment of the gamma beam towards the target,
- ✓ to ensure alignment of the target and its support before starting the experiments,
- ✓ to be able to provide automatic mechanical alignment of the gamma beam based on remote control.

The minimum performances required are:

- ✓ the accuracy of the target alignment system must not exceed 0.5 mm relative to the beam length,
- ✓ the system must detect the gamma beam ray and align the IC-NRF, with the target, to a minimum resolution of 10μm,
- ✓ gamma photons must be detected in the 2 to 20 MeV range by the gamma detector;
- ✓ alignment system components should not be influenced by the gamma rays and should not accelerate aging in interaction with the gamma flux.

The considered alignment system uses a gamma beam detection system providing information with a data acquisition or image capture device. The digital camera contains, in the front of camera, a visible phase gamma beam converter.

In order to be able to ensure the precision of the alignment system, it is necessary to know the vibration response of the beam where the target is located (in this area the gamma beam act).

2. Model and Method

Mathematical modeling of vibrations using the finite element method offers a fast and convenient way to obtain approximate solutions for any type of engineering problems, taking into account the fact that the response of most systems to external actions is extremely difficult, if not impossible to interpret based on a classical mathematical algorithm.

The process of a dynamic analysis represented in Fig. 2 involves a staged analysis of a structure. As can be seen, the input data to be established are the external loads, the geometry of the structure to be analyzed and then the definition of the finite element model. A next step consists in defining the types of dynamic analysis that should be performed according to the goal pursued. These types of dynamic analysis can be: eigenmode analysis, frequency response analysis, transient response analysis, spectral response analysis, random response analysis, etc.

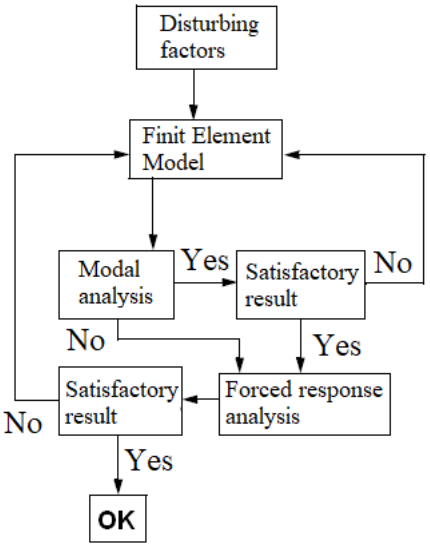

Fig.2: The process of dynamic analysis by numerical methods

In the framework of the forced vibration analyzes carried out on the IC-NRF system described in the previous chapter, the determination of the structural response of the gamma wave guiding element was sought, under the action of a unitary harmonic excitation applied to the base. As shown in Fig. 2, the process of a dynamic analysis first involves the determination of the eigenmodes of vibration, eigenfrequencies and eigenvectors. Later, by knowing the behavior from the point of view of free vibrations, it will be possible to obtain forced response. The gamma-ray guide element shown in Figure 1 can be considered in the case of an analytical calculation equivalent to a cantilever variable cross-section bar of constant thickness along its entire length. For this equivalent system presented in Fig. 3, the equations underlying the determination of the eigenmodes of vibration, the eigenfrequencies are the Euler Bernoulli equations [8].

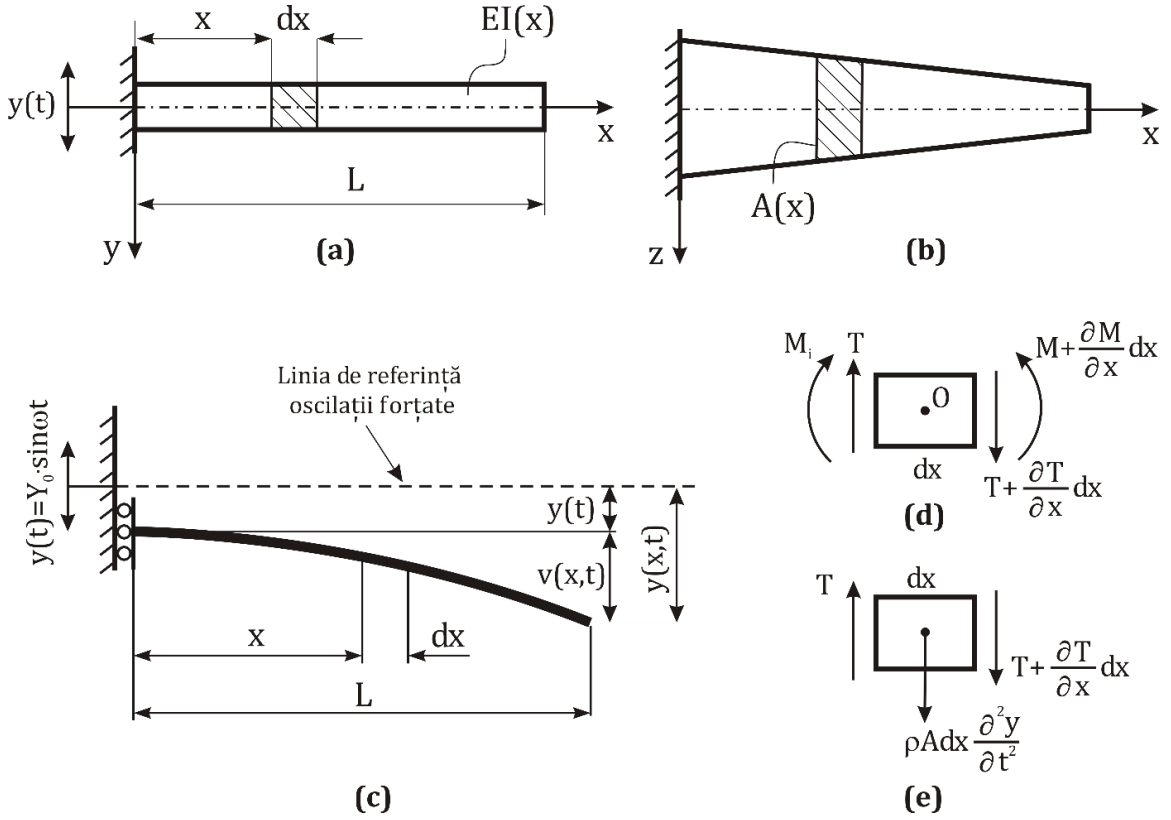

Fig.3: Cantilever beam structure with variable cross-section

Transverse vibrations of bar structures represent a problem in the field of vibrations of continuous systems. The beam in Fig. 3 has a variable cross-section along its axis, its thickness is constant, the bending stiffness modulus is variable along its length, and the material characterized by density ρ will have mass per unit length A. The displacement of a point of beam under displacement-type harmonic excitation is expressed in Eq. (1):

$$y(x,t) = v(x,t) + y(t) \tag{1}$$

where $v(x,t)$ represents the arrow of the bar under the action of its own weight, y(t) is the displacement of the exciting base, and $y(x,t)$ represents the total displacement of the beam. Considering a sinusoidal harmonic motion, it is possible to define it by the law: $y(t) = Y_0 \sin(\omega t)$, where ω is the circular frequency of the harmonic forced vibration, and Y_0 represents the amplitude of the displacement.

Figs. 3, d and 3, e show the forces and moments acting on an infinitesimal element detached from the bar. Equilibrium equations of forces and moments will be written as follows:

- Moment equilibrium equation written on the element of length dx, from Figure 3, d:

$$M + T\frac{dx}{2} + T\frac{dx}{2} + \frac{\partial T}{\partial x}\frac{dx}{2} - M - \frac{\partial M}{\partial x}dx = 0 \quad \Rightarrow \quad Tdx = \frac{\partial M}{\partial x}dx$$

from which a dependence relation between shear forces and bending moments will be obtained, relation (2):

$$T = \frac{\partial M}{\partial x} \tag{2}$$

- The forces balance equation written on the element of length dx, from Fig. 3, e:

Based on the differential equation of the average deformed fiber we can express the bending moment as a function of stiffness [9]:

$$M = -EI(x)\frac{\partial^2 v(x,t)}{\partial x^2} \quad \Rightarrow \quad \frac{\partial^2 M}{\partial x^2} = -EI(x)\frac{\partial^4 v(x,t)}{\partial x^4} \quad .$$

Finally, the general equation of transverse vibrations of a cantilever bar will be obtained:

$$\frac{\partial^4 v(x,t)}{\partial x^4} + \frac{\rho A(x)}{EI(x)}\frac{\partial^2 y(x,t)}{\partial t^2} = 0 \quad . \tag{3}$$

Taking into account (1), it will be obtained:

$$\frac{\partial^4 v(x,t)}{\partial x^4} + \frac{\rho A(x)}{EI(x)}\frac{\partial^2 v(x,t)}{\partial t^2} = -\frac{\rho A(x)}{EI(x)}\frac{\partial^2 y(t)}{\partial t^2} \tag{4}$$

To obtain the eigenmodes of vibration, the homogeneous equation of equation (4) will have to be solved:

$$\frac{\partial^4 v(x,t)}{\partial x^4} + \frac{\rho A(x)}{EI(x)}\frac{\partial^2 v(x,t)}{\partial t^2} = 0 \tag{5}$$

The solution of equation (5) is of the form [10] :

$$v(x,t) = Y(x)\left(B_1 \sin\omega t + B_2 \cos\omega t\right) \tag{6}$$

- Y(x) is a function that defines the vibration mode. By inserting (6) into (5) and after performing the 2nd and 4th order derivatives, we will obtain:

$$\frac{\partial^4 Y}{\partial x^2} - \frac{\rho A}{EI}\omega^2 Y = 0 \quad \Rightarrow \quad \frac{\partial^4 Y}{\partial x^2} = \frac{\rho A}{EI}\omega^2 Y = \beta^4 Y \quad , \tag{7}$$

where $\beta^4 = \frac{\rho A}{EI}\omega^2$ represents the equation of the beam that has the general solution of the type:

$$Y(x) = C_1 e^{\beta x} + C_2 e^{-\beta x} + C_3 e^{i\beta x} + C_4 e^{-i\beta x}$$

or:

$$\begin{aligned} Y(x) &= C_1\left[\cos(\beta x) + \cosh(\beta x)\right] + C_2\left[\cos(\beta x) - \cosh(\beta x)\right] \\ &+ C_3\left[\sin(\beta x) + \sinh(\beta x)\right] + C_4\left[\sin(\beta x) - \sinh(\beta x)\right] \quad . \end{aligned}$$

The coefficients C_1, C_2, C_3, C_4 will be determined from the boundary conditions:

$$x = 0 \quad \Rightarrow \quad \begin{cases} v = 0 \\ \dfrac{dv}{dx} = 0 \end{cases} \quad \Rightarrow \quad \begin{cases} Y(0) = 0 \\ Y'(0) = 0 \end{cases} \quad \Rightarrow \quad \begin{cases} C_1 = 0 \\ C_3 = 0 \end{cases} \quad .$$

$$x = L \quad \Rightarrow \quad \begin{cases} T = 0 \\ M = 0 \end{cases} \quad \Rightarrow \quad \begin{cases} Y''(L) = 0 \\ Y'''(L) = 0 \end{cases} \quad \Rightarrow \quad \begin{cases} C_2\left[\cos(\beta L) + \cosh(\beta L)\right] + C_4\left[\sin(\beta L) + \sinh(\beta L)\right] = 0 \\ C_2\left[-\sin(\beta L) + \sin sh(\beta L)\right] + C_4\left[\cos(\beta L) + \cosh(\beta L)\right] = 0 \end{cases} .$$

In matrix form, the equations obtained from the boundary conditions for x=L are:

$$\begin{bmatrix} \cos(\beta L)+\cosh(\beta L) & \sin(\beta L)+\sinh(\beta L) \\ -\sin(\beta L)+\sinh(\beta L) & \cos(\beta L)+\cosh(\beta L) \end{bmatrix} \begin{Bmatrix} C_2 \\ C_4 \end{Bmatrix} = \begin{Bmatrix} 0 \\ 0 \end{Bmatrix} \tag{8}$$

The matrix system (8) has non-trivial solutions, if and only if its determinant is zero. Writing this condition will give the following transcendental equation:

$$\cos(\beta L)\cosh(\beta L) = -1 \ . \tag{9}$$

In Table 1 the first four solution are presented. They offer the first four eigenmodes of vibration.
From (8) we obtain the dependence between the constants C_2 and C_4.

$$C_4 = -\frac{\cos(\beta L)+\cosh(\beta L)}{\sin(\beta L)+\sinh(\beta L)} C_2 \ . \tag{10}$$

The equation that gives the shape of the eigenmode is:

$$Y_i(x) = \left[\cos(\beta_i x)-\cosh(\beta_i x)\right] - \frac{\cos(\beta_i L)+\cosh(\beta_i L)}{\sin(\beta_i L)+\sinh(\beta_i L)}\left[\sin(\beta_i x)-\sinh(\beta_i x)\right] \tag{11}$$

.

Table 1: Calculation of parameters for the equation of the beam

Solution no. i	$\beta_i L$
1	1.8751
2	4.6941
3	7.8547
4	10.9956

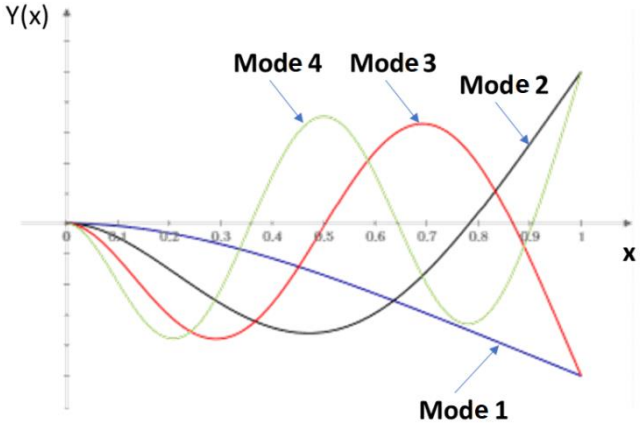

Fig. 4: Shape of eigenmodes for a cantilever beam

Based on the determined natural modes of vibration (Fig.4), the vibration response of the structure to the action of a disturbance such as a harmonic excitation applied to the base is to be determined.

Eq.(4), which is the equation on the basis of which the forced response is obtained, can also be expressed as:

$$EI\frac{\partial^4 v(x,t)}{\partial x^4} + \rho A\frac{\partial^2 v(x,t)}{\partial x^2} = f(x,y) \ . \tag{12}$$

Taking into account the fact that the displacement-type base excitation is $y = Y_0 \sin(\omega t)$, the force function in the right-hand member becomes:

$$f(x,y) = \rho A \omega^2 Y_0 \sin(\omega t) \tag{13}$$

The dynamic system described for equation 12 is presented in Fig. 5.

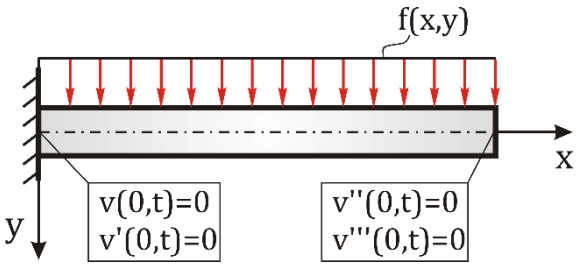

Fig.5: Cantilever beam with boundary conditions

The relative transverse displacements of any point located on the beam, in relation to the base, is considered to be under the form:

$$v(x,y) = \sum_{i=1}^{4} Y_i(x) q_i(t) \tag{14}$$

where, $Y_i(x)$ is the normalized eigenmodes function. Substituting (14) into (12), multiplying the resulting expression by $Y_j(x)$ and integrating all the terms over the length of the bar, the relation will be obtained:

$$\left[EI \int_0^L \frac{\partial^4 Y_i(x)}{\partial x^4} Y_j(x) dx \right] q_i + \left[\rho A \int_0^L Y_i(x) Y_j(x) dx \right] \ddot{q}_i = \int_0^L Y_i(x) f(x,y) dx \quad . \tag{15}$$

The eigenmode shapes are orthonormal, conditions expressed by the formulas [11]:

$$EI \int_0^L \frac{\partial^4 Y_i(x)}{\partial x^4} Y_j(x) dx = \omega_i^2 \delta_{ij} \quad ; \quad \rho A \int_0^L Y_i(x) Y_j(x) dx = \delta_{ij} \quad . \tag{16}$$

where δ_{ij} is the Delta Kronecker function shown in (17):

$$\delta_{ij} = \begin{cases} 1 & if \quad i = j \\ 0 & if \quad i \neq j \end{cases} \quad . \tag{17}$$

Substituting (16) into (15) yields:

$$\omega_i^2 q_i + \ddot{q}_i = Q_i(t) \quad , \tag{18}$$

with $Q_i(t)$:

$$Q_i(t) = \int_0^L Y_i(x) f(x,y) dx \, . \tag{19}$$

The solution of equation (18) is [12]:

$$q_i(t) = a_i \sin(\omega_i t) + b_i \cos(\omega_i t) + \int_0^t Q_i(\tau) h(t-\tau) d\tau \, . \tag{20}$$

The third term in (20) represents the integral of the convolution [11], and the term h(tt) represents the response of an impulse unit given by the relation:

$$h(t-\tau)=\frac{1}{\omega_i}\sin\omega_i(t-\tau)\ . \tag{21}$$

Substituting (21) and (18) into the convolution integral will result:

$$\int_0^t Q_i(\tau)h(t-\tau)d\tau=\frac{\rho A\omega^2 Y_0}{\omega_i}\int_0^L Y_i(x)dx\int_0^t \sin(\omega t)\sin\left[\omega_i(t-\tau)d\tau\right]=F_1^iF_2^i\ , \tag{22}$$

with F_1^i and F_2^i defined by the relations:

$$F_1^i=\int_0^L Y_i(x)dx\quad , \tag{23}$$

$$F_2^i=\frac{\rho A\omega^2 Y_0}{\omega_i}\int_0^t \sin(\omega t)\sin\left[\omega_i(t-\tau)d\tau\right]=\frac{\rho A\omega^2 Y_0}{\omega_i}\frac{\omega\sin(\omega_i t)-\omega_i\sin\omega t}{\omega^2-\omega_i^2}\quad .$$

The coefficients a_i and b_i in Eq.(20) are determined from the boundary conditions (initial conditions in our case):

$$v(x,0)=0\quad ,\quad \dot v(x,0)=0\quad . \tag{24}$$

So, the general form of Eq.(20) will be:

$$q_i(t)=\frac{\dot q_{i0}}{\omega_i}\sin(\omega_i t)+q_{i0}\cos(\omega_i t)+\frac{\rho A\omega^2 Y_0}{\omega_i}\frac{\omega\sin(\omega_i t)-\omega_i\sin\omega t}{\omega^2-\omega_i^2}\int_0^L Y_i(x)dx \tag{25}$$

where, the terms q_{i0} and $\dot q_{i0}$ are [13]:

$$q_{i0}=\int_0^L \rho A v(x,0)Y_i(x)dx\quad ,\quad \dot q_{i0}=\int_0^L \rho A\dot v(x,0)Y_i(x)dx \tag{26}$$

The total displacement of the bar under harmonic excitation of the base will be:

$$y(x,t)=y(t)+\sum_{i=1}^{4}Y_i(x)q_i(t) \tag{27}$$

In general, force response approaches are done in the frequency domain using Fourier transforms due to the much reduced volume of calculations. In the last decade, most forced response calculations are made based on information obtained from the free vibration calculation such as: modal participation factors, effective modal mass factors and cumulative mass.

Finite Element Methods represents another way to obtain the motion equations and finaly the numerical response of the vibration behavior of a system [5, 14-21]. But this methods offer only numerical results and not a qualitative image of the system behavior.

Every structure tends to vibrate with a response that is the sum of a certain set of harmonic vibration with the natural frequencies (eigenfrequencis). For every eigenfrequency there is an eigenmode shape. The modal participation factor represents a measure of how much a particular mode contributes to the overall structure's response if there is an excitation in an arbitrary direction.

In vibration analysis, there are two related topics that must be considered. These are the resonance and modal participation. In a resonant regime, the excitation amplifies the mode. Obviously, large displacements can appear. On the other hand, it is possible for the excitation frequency to match a natural frequency (ie a resonant condition)

but the participation factor of the mode is close to zero which means that little energy will enter with that mode and a response will be negligible dynamic.

Modal participation factors are scalars that measure the interaction between the responses given by the eigenmodes of vibration and the direction of excitation in a defined reference frame. Higher values of these factors indicate a more significant contribution to the dynamic response.

The cumulative mass for mode '*n*' is the sum of the effective mass factors for modes 1 through '*n*'. A common rule of thumb for linear dynamic analysis is to include enough modes so that the cumulative mass is at least 80% in the predominant direction of the excitation vibration.

For a bar of length *L* and mass per unit length $\rho A(x)$, the modal participation factors are calculated with the relation [22, 23]:

$$\Gamma_i(x) = \int_0^L m(x) Y_i(x) dx = \int_0^L \rho A(x) Y_i(x) dx \tag{28}$$

where $Y_i(x)$ are the eigenvectors obtained by mass normalization, calculated with (11).

The generalized modal mass and the effective modal mass on each mode are calculated with the following relations [22, 23]:

$$\hat{m}_i = \int_0^L m(x) Y_i^2(x) dx = 1 \quad ; \quad m_{eff,i} = \frac{\left[\int_0^L m(x) Y_i(x) dx\right]^2}{\hat{m}_i} = \Gamma_i^2 \quad . \tag{29}$$

Since the normalization of the eigenvectors is done as a function of the mass, the generalized modal mass $\hat{m}_i$ has unit value.

The determination of the forced response for a cantilever bar excited at the base according to a harmonic law of unit amplitude and taking into account the damping expressed by the fraction of the critical damping, is given in (30), (see [14]) .

$$Y(x,\omega) = \ddot{y}(\omega) \sum_{i=1}^{4} \frac{-\Gamma_i Y_i(x)}{\left(\omega_i^2 - \omega^2\right) + 2j\xi_i \omega \omega_i} \tag{30}$$

$Y(x,\omega)$ – the relative displacement of the beam with respect to the base according to the excitation pulse;

$\ddot{y}(\omega)$ - excitation acceleration converted from time to frequency;

Γ_i - the modal participation factor specific to each mode;

$Y_i(x)$ – the eigenvectors normalized on the basis of the mass, specific to each eigenmode;

□□– excitation pulsation;

□□ – the natural pulsation of each mode;

ξ_i - the fraction of the critical damping.

3. Results

The finite element model, shown in Fig. 6 was discretized with SHELL finite elements with four corner nodes, a node having 6 nodal degrees of freedom. Since the field of use of the analyzed element requires a high precision, the frequency range for which the free vibrations were studied was considered between 0 and 1000 Hz. In the modal analysis, the eigenmodes specific to the movement of the guiding element in the direction of excitation were mainly followed. The main parameters monitored for each mode in the free vibration analysis were: natural frequency, modal participation factors, effective modal mass and eigenmode shape.

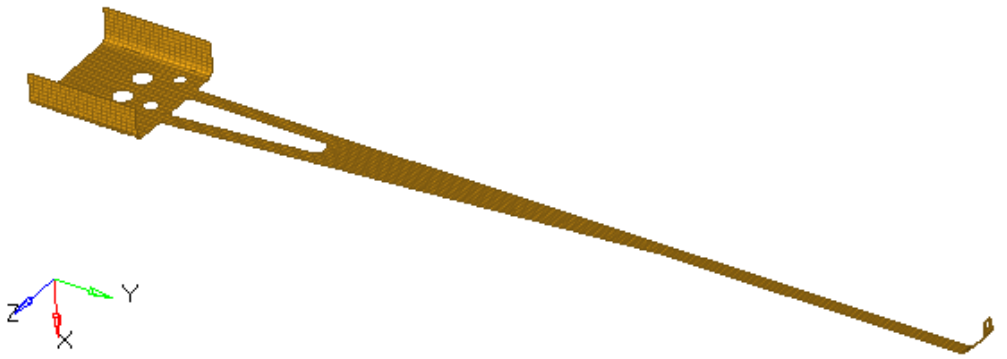

Fig.6: Finite element model of the gamma beam ray guide element

The material from which the guide beam is made is a steel with the following properties: Young's modulus E = 21,000 MPa, Poisson' s ratio, $\boldsymbol{\nu = 0.3}$ and density $\boldsymbol{\rho = 7}$,860 kg/m^3. The thickness of the beam is 2 mm, and its mass is 93.28 grams.

Within the framework of finite element analyzes (FEA) it was aimed to determine how large the displacement of the target will be when the vibration amplitude in the base is unitary [24, 25].

In the frequency range established for free vibration analysis, 27 natural modes were obtained. In tables 2,3 and 4 you can see normalized modal participation factors and the effective modal mass for the first 14 eigenmodes of vibration.

Table 2: Normalized participation modal factors

Eigenmode	Frequency	Translation			Rotation		
	[Hz]	X	Y	Z	RX	RY	RZ
Mode 1	19.254	1	0.0042	0.000	0.0000	0.0863	1
Mode 2	85.658	0.6971	0.0101	0.001	0.0012	0.2283	0.3882
Mode 3	121.42	0.0012	0.0134	0.8782	1	0.7324	0.000
Mode 4	237.96	0.4309	0.0212	0.0020	0.0021	0.2671	0.2023
Mode 5	448.12	0.0128	0.0638	1	0.7492	1	0.0081
Mode 6	463.21	0.3011	0.0196	0.0481	0.0364	0.1512	0.1343
Mode 7	770.93	0.2243	0.0391	0.0602	0.0364	0.1621	0.0944
Mode 8	820.62	0.0212	0.0391	0.6797	0.3871	0.3929	0.0072
Mode 9	1010.1	0.0071	0.0142	0.4864	0.2458	0.7633	0.0031
Mode 10	1151.8	0.1808	0.0352	0.0062	0.0039	0.1143	0.0765
Mode 11	1378.2	0.000	0.000	-0.0010	-0.1591	0.0011	0.0021
Mode 12	1601.2	-0.001	0.000	0.0000	0.0021	-0.0061	0.1112
Mode 13	1715.7	0.000	0.000	-0.0010	-0.0982	0.0183	-0.0021
Mode 14	2101.4	-0.001	0.000	0.0000	-0.0081	-0.0071	0.1049

Table 3: Effective modal mass

Eigen mode	Frequency	Translation			Rotation		
	[Hz]	X	Y	Z	RX	RY	RZ

Mode 1	19.254	2.32×10^{-5}	2.60×10^{-10}	1.73×10^{-13}	3.94×10^{-8}	2.77×10^{-5}	3.01
Mode 2	85.658	1.13×10^{-5}	2.07×10^{-9}	1.41×10^{-11}	2.57×10^{-6}	1.94×10^{-4}	4.53×10^{-1}
Mode 3	121.42	4.73×10^{-11}	3.63×10^{-9}	1.25×10^{-5}	2.04	2.00×10^{-3}	4.01×10^{-7}
Mode 4	237.96	4.30×10^{-6}	8.53×10^{-9}	6.73×10^{-11}	8.77×10^{-6}	2.66×10^{-4}	1.22×10^{-1}
Mode 5	448.12	3.75×10^{-9}	8.14×10^{-8}	1.62×10^{-5}	1.15	3.73×10^{-3}	1.89×10^{-4}
Mode 6	463.21	2.11×10^{-6}	8.03×10^{-9}	3.69×10^{-8}	2.58×10^{-3}	8.46×10^{-5}	5.37×10^{-2}
Mode 7	770.93	1.16×10^{-6}	2.96×10^{-8}	5.92×10^{-8}	2.69×10^{-3}	9.77×10^{-5}	2.65×10^{-2}
Mode 8	820.62	9.84×10^{-9}	3.04×10^{-8}	7.49×10^{-6}	3.06×10^{-1}	5.76×10^{-4}	1.66×10^{-4}
Mode 9	1010.1	1.24×10^{-9}	4.13×10^{-9}	3.82×10^{-6}	1.23×10^{-1}	2.17×10^{-3}	3.21×10^{-5}
Mode 10	1151.8	7.60×10^{-7}	2.43×10^{-8}	5.72×10^{-10}	2.88×10^{-5}	4.88×10^{-5}	1.79×10^{-2}
Mode 11	1378.2	2.64×10^{-10}	5.54×10^{-9}	1.19×10^{-6}	2.52×10^{-2}	1.96×10^{-6}	4.05×10^{-6}
Mode 12	1601.2	5.84×10^{-7}	1.26×10^{-7}	1.06×10^{-13}	5.59×10^{-6}	4.22×10^{-5}	1.23×10^{-2}
Mode 13	1715.7	6.93×10^{-10}	6.52×10^{-11}	6.04×10^{-7}	9.62×10^{-3}	3.27×10^{-4}	2.36×10^{-6}
Mode 14	2101.4	4.09×10^{-5}	2.46×10^{-8}	1.43×10^{-9}	5.76×10^{-5}	4.43×10^{-5}	1.10×10^{-2}
TOTAL		9.32×10^{-5}	9.32×10^{-5}	9.32×10^{-5}	1.24x10	$1.89\times10^{+3}$	7.03

Table 4: Effective modal mass (percentage)

Eigenmode	Translation [%]			Rotation [%]		
	X	Y	Z	RX	RY	RZ
Mode 1	24.87	0.00	0.00	0.00	0.00	42.75
Mode 2	12.07	0.00	0.00	0.00	0.00	6.44
Mode 3	0.00	0.00	13.39	16.48	0.00	0.00
Mode 4	4.61	0.01	0.00	0.00	0.00	1.74
Mode 5	0.00	0.09	17.36	9.24	0.00	0.00
Mode 6	2.26	0.01	0.04	0.02	0.00	0.76
Mode 7	1.24	0.03	0.06	0.02	0.00	0.38
Mode 8	0.01	0.03	8.02	2.47	0.00	0.00
Mode 9	0.00	0.00	4.09	1.00	0.00	0.00
Mode 10	0.81	0.03	0.00	0.00	0.00	0.25
Mode 11	0.00	0.01	1.28	0.20	0.00	0.00
Mode 12	0.63	0.14	0.00	0.00	0.00	0.18
Mode 13	0.00	0.00	0.65	0.08	0.00	0.00
Mode 14	0.44	0.03	0.00	0.00	0.00	0.16

In Tab. 4, the percentage effective modal masses were highlighted for values greater than 2%. Since the applied excitation is oriented along the global axis X of the reference system which can be seen in Fig. 6, the eigenmodes of interest from the point of view of the force response study are 1, 2, 4, 6, specifically the first four bending modes with respect to the Z axis.

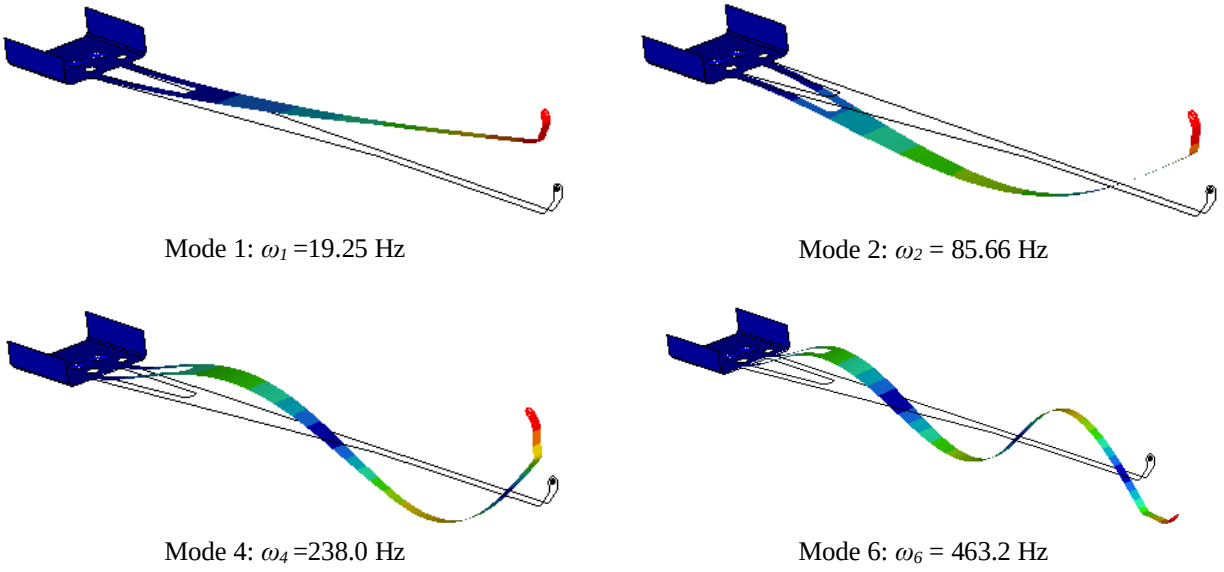

Fig. 7: Finite Element Model and eigenmodes of vibration

Based on the percentage values of the effective modal masses obtained from the analysis, it can be concluded that the effective modal mass of mode 1 presents the highest values which means that a large part of the bending vibration energy is given by this mode. This is highlighted by both the high percentage of translation along the X axis (24.87%) and the high percentage obtained on rotation around the Z axis (42.75%). The same can be said for mode 2.

Modes 3, 5, 8 and 9 are also bending eigenmodes but for an excitation acting in a direction perpendicular to the plane in which the bending vibration specific to these modes occurs and the forced response will not amplify the vibration.

In Fig. 8 shows the variation of the forced displacement response for the free end of the gamma beam guide element.

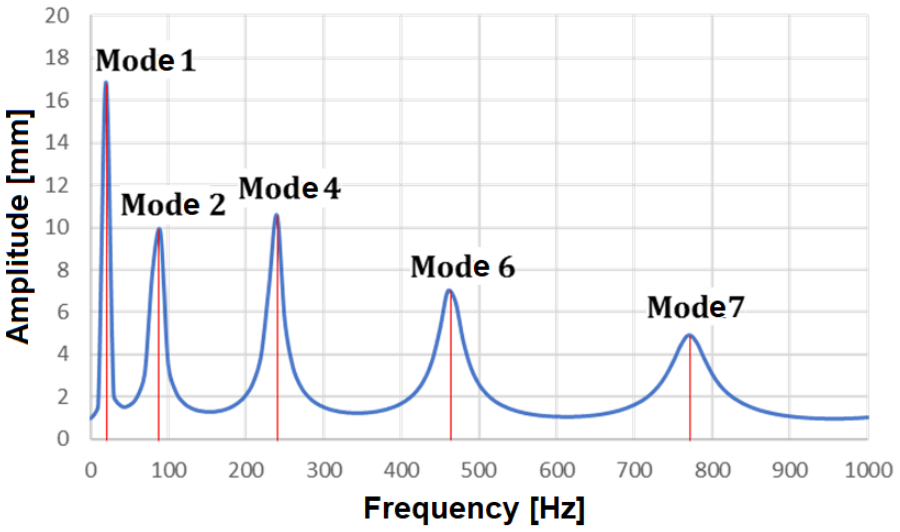

Fig. 9. Forced free-end response for the gamma guide element

4. Conclusions

The free and forced vibration analysis performed for the gamma wave guide beam illustrates some important aspects that must be considered when designing the final solution of this guide element.

Based on the graph obtained from the forced response analysis, it can be observed that the guiding element presents a rather high flexibility, and this is highlighted by the amplitude response obtained on the natural modes of vibration. As can be seen from the modal participation factors, respectively the effective modal mass, mode 1 can be considered the most influential for the response obtained. Depending on this way, proposals can be made to improve the constructive solution analyzed, which presuppose a redesign of the constructive form so that it leads to a maximum vibration amplitude as low as possible.

References

[1] G. Wormser, C. Barty, R. Hajima, P. Boni, D. Bucurescu, A. Buta, G. Cata-Danil, R. Chapman, F. Constantin, V. Corcalciuc, L. Csige, L. Cune, B. Dietz, M. Dima, G. Dollinger, D. Dudu, M. Zepf, 2010, *The White Book of ELI Nuclear Physics Bucharest-Magurele, Romania*,

[2] O. Adriani, S. Albergo, D. Alesini, M. P. Anania, D. Angal-Kalinin, P. Antici, B. Alberto, R. Bedogni, M. Bellaveglia, C. Biscari, N. Bliss, R. Boni, M. Boscolo, F. Broggi, P. Cardarelli, K. Cassou, M. Castellano, L. Catani, I. Chaikovska, F. Zomer, Technical Design Report EuroGammaS proposal for the ELI-NP Gamma beam System, 07/14, 2014.

[3] D. Habs, T. Tajima, N. Zamfir, Extreme Light Infrastructure–Nuclear Physics (ELI–NP): New Horizons for Photon Physics in Europe, *Nuclear Physics News,* Vol. 21, pp. 23-29, 02/28, 2011.

[4] N. Zamfir, Nuclear Physics with 10 PW laser beams at Extreme Light Infrastructure – Nuclear Physics (ELI-NP), *The European Physical Journal Special Topics,* Vol. 223, pp. 1221-1227, 05/01, 2014.

[5] S. Vlase, Elimination of lagrangian multipliers, *Mechanics Research Communications,* Vol. 14, No. 1, pp. 17-22, 1987.

[6] I. Negrean, A. Crisan, S. Vlase, A New Approach in Analytical Dynamics of Mechanical Systems, *Symmetry,* Vol. 12, pp. 95, 01/03, 2020.

[7] Y. Khulief, On the finite element dynamic analysis of flexible mechanisms, *Computer Methods in Applied Mechanics and Engineering,* Vol. 97, No. 1, pp. 23-32, 1992.

[8] S. Timoshenko, S. Woinowsky-Krieger, 1959, *Theory of plates and shells*, McGraw-hill New York,

[9] C. Itu, 2019, *Strength of Materials in Mechanical Engineering*, Transilvania University Publishing House, Brașov

[10] C. Beards, 1995, *Engineering vibration analysis with application to control systems*, Elsevier,

[11] W. Thomson, 2018, *Theory of vibration with applications*, CrC Press,

[12] D. G. Zill, M. R. Cullen, W. S. Wright, 1997, *Differential equations with boundary-value problems*, Brooks/Cole Publishing Company,

[13] W. Sun, Y. Liu, H. Li, D. Pan, Determination of the response distributions of cantilever beam under sinusoidal base excitation, *Journal of Physics Conference Series,* Vol. 448, pp. 2010, 07/01, 2013.

[14] S. Vlase, I. Negrean, M. Marin, S. Năstac, Kane's Method-Based Simulation and Modeling Robots with Elastic Elements, Using Finite Element Method, *Mathematics,* Vol. 8, No. 5, pp. 805, 2020.

[15] M. Marin, A temporally evolutionary equation in elasticity of micropolar bodies with voids, *Bull. Ser. Appl. Math. Phys,* Vol. 60, No. 3, 1998.

[16] M. Marin, A. Hobiny, I. Abbas, The Effects of Fractional Time Derivatives in Porothermoelastic Materials Using Finite Element Method, *Mathematics,* Vol. 9, pp. 1606, 07/07, 2021.

[17] M. Marin, A. Seadawy, S. Vlase, A. Chirila, On mixed problem in thermoelasticity of type III for Cosserat media, *Journal of Taibah University for Science,* Vol. 16, No. 1, pp. 1264-1274, 2022.

[18] M. L. Scutaru, S. Vlase, M. Marin, Analytical mechanics methods in finite element analysis of multibody elastic system, *Boundary Value Problems,* Vol. 2023, No. 1, pp. 97, 2023.

[19] M. L. Scutaru, M. Marin, S. Vlase, Dynamic Absorption of Vibration in a Multi Degree of Freedom Elastic System, *Mathematics,* Vol. 10, No. 21, pp. 4045, 2022.

[20] P. Bratu, C. Dobrescu, N. Marilena Cristina, Dynamic Response Control of Linear Viscoelastic Materials as Resonant Composite Rheological Models, Vol. 20, pp. 73-77, 10/02, 2023.

[21] C. RUGINA, T. SIRETEANU, V. CHIROIU, L. MUNTEANU, M. Ana-Maria, Experimental and Numerical Simulation of a Multilevel Structure Behaviour Subjected to Transient Loads, *Romanian Journal of Acoustics and Vibration,* Vol. 20, No. 2, pp. 147-156, 2023.
[22] T. Irvine, An Introduction to Shock and Vibration Response Spectra, *Partnership with enDAQ. com*, 2018.
[23] T. Irvine, Effective modal mass and modal participation factors, *Available on the web on site: http://www. vibrationdata. com/tutorials2/ModalMass. pdf.(last access on march 7 2007)*, 2013.
[24] J. P. Den Hartog, 1987, *Advanced strength of materials*, Courier Corporation,
[25] M. L. Scutaru, S. Vlase, Some properties of motion equations describing the nonlinear dynamical response of a multibody system with flexible elements, *Journal of Applied Mathematics,* Vol. 2012, 2012.